Modeling neuronal current MRI signal with human neuron

Q. Luo[1], and J-H. Gao[1]
[1]The University of Chicago, Chicago, IL, United States

Introduction

In the past, magnitude of neuronal current MRI (ncMRI) signal was estimated based on the real morphological and physiological properties of neuron in animals, such as monkey[1] and rat[2]. Their results[1, 2] indicated that the ncMRI signal change can vary significantly between different animal species. In this study, we extend the ncMRI model to human brain for first time. The morphological and physiological properties of human cortical pyramidal neurons are used in the calculation of the ncMRI signal. Also, the variation of neuronal density in different cortical layers (layers I-VI) is considered to further improve the accuracy of simulation. The results from this modeling work will provide valuable information for assessing the feasibility of ncMRI in human subjects.

Methods

The ncMRI signal is simulated in the following procedures: (1) Simulate the ion currents in a single firing neuron and the neuronal magnetic fields (NMFs) generated by the currents. (2) Calculate the NMFs in a cortical tissue based on the NMFs of the single neuron. (3) Simulate the ncMRI signal changes in magnitude and phase in the cortical tissue using the typical gradient echo EPI pulse sequence.

Ion currents and NMFs of a single neuron: The ncMRI signal simulation starts with the calculation of ion currents in two firing neurons (neuron 1 and 2). These neurons are 3-D constructed from layer III of prefrontal cortex[3] and auditory cortex[4], respectively. Neuron 1 and 2 share the same passive membrane parameters: membrane resistivity = 15 Ω·cm^2, intracellular resistance = 245 Ω·cm and membrane capacitance = 0.76 μF/cm^2. Typical active membrane properties of pyramidal neuron[5] are applied to both neurons. The stimulation to the neurons is simulated by 25 excitatory synaptic inputs, which are randomly located in the dendrites and generated synchronously at a frequency of 40 Hz. Each synaptic event is modeled as a double-exponential function with peak conductance = 0.5 nS, rise/decay time constant = 0.4/1 ms and reversal potential = 0 mV. The calculation of ion currents is performed using the NEURON simulator. With the spatial distribution of ion currents, the components of NMFs parallel to B_0 are calculated according to Biot-Savart law. B_0 and neuronal length axis are assumed to be along z and y axis, respectively. The origin is set at the soma.

NMFs in cortical tissue: Based on the NMFs of the single neurons (neuron 1 and 2), the NMFs are simulated in two activated brain tissues (tissue 1 and 2), which are composed of multiple parallel copies of neuron 1 and 2, respectively. Each tissue has a surface area of 3×3 mm^2 and is 2.5 mm thick. The cortical surface is parallel to x-z plane and y-axis is along the direction of thickness (parallel to the neuronal length axis). The tissue is divided into six cortical layers (layers I-VI) along the thickness direction. The thickness and neuron density of each layer are obtained from the previous measurement results[6], and the neurons are randomly distributed in the tissue. The firing rate of neuron is assumed to vary in 0-25%, which covers the range of firing rate for different types of neuronal activity (i.e., evoked, spontaneous, and epileptic). The z-component (along B_0) of NMFs in tissue 1 and 2 are calculated by superimposing the NMFs of individual firing neurons.

ncMRI signal in cortical tissue: The corresponding ncMRI signal changes are calculated using the following imaging parameters: gradient echo EPI pulse sequence, TE = 0-50 ms (interval = 1 ms), and voxel size = 1 × 1 × 1 mm^3. The calculation method has been described previously[7]. Since ncMRI signal changes depend on relative position of voxel in the tissue, the signal changes are calculated for all possible voxel positions to find out the maximum signal change.

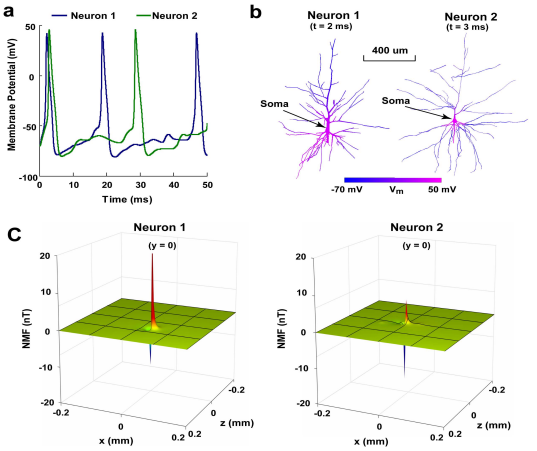

Fig. 1 Neuronal currents and NMFs of single neuron.

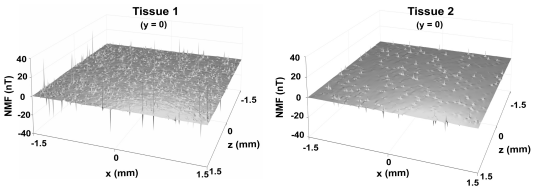

Fig. 2 NMFs in cortical tissue 1 and 2 at plane y = 0 (firing neuron density = 800 neurons/mm^3).

Results and Discussion

Figs. 1a and 2b show the time courses of membrane potentials at soma and the spatial distribution of membrane potentials in neuron 1 and 2 at potential peak time (t = 2 and 3 ms for neuron 1 and 2), respectively. The distribution of the component of NMF along z-axis (parallel to B_0) at plane y = 0 is shown in Fig. 1c. It can be seen that the amplitude and polarity of the corresponding NMFs vary with spatial locations. The NMFs around neuron 1/neuron 2 reach to the maximum at the soma and the maximum amplitude is 18/12 nT approximately. The NMFs decay rapidly with the increase of distance from the neuron. The NMF at a point is below 0.1 nT when its distance from the soma is larger than 100 μm.

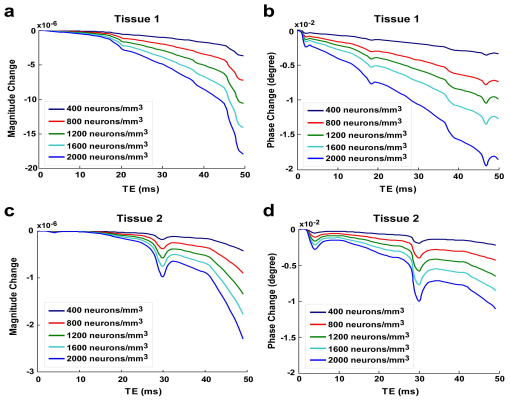

Fig. 3 ncMRI signal changes in activated tissues.

The NMFs in the cortical tissue (tissue 1 and 2) are calculated with different neuron firing rate (= 0-25%, 5% interval), corresponding to average firing neuron density of 0-2000 neurons/mm^3 (interval = 400 neurons/mm^3). It is found that the cortical NMFs are inhomogeneous in space (Fig. 2). The mean (absolute value) and the standard deviation of NMF in the cortical tissue increased with neuron firing rate (firing density).

The ncMRI signal changes in tissue 1 and 2 for different firing neuron densities are shown in Fig. 3. ncMRI magnitude and phase changes increased with TE. For a given TE, the magnitude and phase signals increased with increase in firing neuron density. Considering that the firing neuron density for typical neuronal activity (i.e., evoked, spontaneous, and epileptic activity) is lower than 2000 neurons/mm^3, then the amplitude of ncMRI magnitude/phase changes in tissue 1 (prefrontal cortex) and 2 (auditory cortex) will be up to 1.8×10^{-5}/0.02° and 2.3×10^{-6}/0.01° at TE = 50 ms (Fig. 3). In practice, such a small signal change is difficult to be detected using present MRI technology.

References

1. Blagoev et al. Neuroimage 2007;37:137. 2. Cassara et al., Neuroimage 2008;39:87. 3. Hayes et al. Arch Neurol 1996;53:1277. 4. Benavides-Piccione et al. Cereb Cortex 2005;15:1584. 5. Migliore et al. Nat Rev Neurosci 2002;3:362. 6. Rajkowska et al. Arch Gen Psychiatry 1998;55:215. 7. Konn et al. Magn Reson Med 2003;50:40.